Early detection of cardiac impairment and prediction of right ventricular hypertrophy in patients with connective tissue disease

JIAYAN SHEN[1*], GUANGRONG XIAO[1*], SHUQING FANG[1], HAOHAO YANG[1], ZHEREN ZHAO[1], YUN XU[1], MENG JIANG[2] and SONG ZHONG[1]

[1]Department of Intensive Care Unit, Renhe Hospital, Shanghai 201999, P.R. China; [2]Department of Cardiology, Renji Hospital, Shanghai Jiaotong University, School of Medicine, Shanghai 200127, P.R. China

Received August 14, 2024; Accepted November 29, 2024

DOI: 10.3892/br.2025.1970

Abstract. Progressive right ventricle (RV) failure and death in connective tissue disease (CTD) are related to RV hypertrophy (RVH) and dilation, irrespective of pulmonary arterial hypertension (PAH). Therefore, detecting cardiac impairment before RVH and determining RVH predictors is crucial for timely intervention. The present prospective cohort study aimed to identify cardiac markers that occur before RVH and to investigate predictors of RVH. CTD was diagnosed based on clinical features, laboratory findings and imaging data. The cardiac functions of patients with CTD were evaluated using echocardiography, cardiovascular magnetic resonance (CMR) and multi-modality cardiac imaging studies, including RV wall thickness, systolic functions, late gadolinium enhancement, T1 maps and biventricular strain analysis. A total of 52 patients with CTD with non-right ventricular hypertrophy (non-RVH), 34 patients with RVH and 50 healthy individuals were prospectively included. The impaired cardiac indices in patients with RVH included RV ejection fraction, ventricular dimensions, global myocardial deformation, late gadolinium enhancement and ventricular extracellular volume (ECV). The cardiac death rate did not differ significantly between the RVH and non-RVH groups (P=0.14). Conventional parameters, including serum cardiac markers and the left ventricular ejection fraction, showed no significant changes in the non-RVH group compared with the control group. Regarding fibrosis assessment using CMR, an elevated native T1 value (1,362±72 msec in the non-RVH group vs. 1,268±42 in the control group; P<0.001) and ECV (31±4% in the non-RVH group vs. 25±3% in the control group; P<0.001) were observed. By contrast, T1 myocardium/msec 15 min post-contrast of the left ventricle in the RVH group was significantly decreased compared with that in the non-RVH group, indicating an increase in the extracellular matrix at this stage. RVH was predicted by pulmonary arterial pressure (PAP) in patients in the non-RVH group (t-statistic, 2.84; P=0.01), whereas after RVH presentation, RV end-systolic volume (RVESV) became a progression predictor of RVH (t-statistic, 7.98; P<0.0001). No other cardiac imaging or laboratory findings predicted RVH. To the best of our knowledge, the present study was the first to highlight the non-invasive detection of cardiac tissue impairment using CMR and provide support for cardiac treatment initiation before RVH detection. The predictors of RVH vary with the heart disease stage. PAP in the non-RVH stage and incompetence of RVESV in the RVH stage predicted the progression of RVH. The present study was part of a clinical trial (NCT03271385), which was registered on July 1, 2017, and started on September 1, 2017.

Correspondence to: Dr Meng Jiang, Department of Cardiology, Renji Hospital, Shanghai Jiaotong University, School of Medicine, 160 Pujian Road, Shanghai 200127, P.R. China
E-mail: sjy19850623@163.com

Dr Song Zhong, Department of Intensive Care Unit, Renhe Hospital, 1999 Changjiang West Road, Shanghai 201999, P.R. China
E-mail: zhong19742006@126.com

*Contributed equally

Abbreviations: CMR, cardiovascular magnetic resonance; CTD, connective tissue disease; ECG, electrocardiogram; ECV, ventricular extracellular volume; LGE, late gadolinium enhancement; PAH, pulmonary arterial hypertension; RHC, right heart catheterization; RV, right ventricle; RVH, right ventricular hypertrophy; SLE, systemic lupus erythematosus

Key words: CTD, RVH, ECV, myocardial deformation, CMR

Introduction

Cardiac disease is a leading cause of connective tissue disease (CTD) mortality and has attracted considerable attention (1). Most patients with CTD present with nonspecific cardiac symptoms, normal electrocardiogram (ECG) findings and a preserved left ventricle (LV) ejection fraction (2,3). Therefore, they do not receive an early cardiac diagnosis. Pulmonary arterial hypertension (PAH), right ventricle (RV) dilatation and hypertrophy are common complications of CTD with critical consequences (4). The prevalence of CTD-associated PAH based on right heart catheterization (RHC) is estimated to be as high as 13% (5). The incidence of systemic lupus erythematosus (SLE)-associated PAH ranges between 0.5 and 43%, and this leads to compromised RV functions (6). The prevalence of PAH in patients with scleroderma is between

5 and 12% (7). Among patients with mixed CTD, 20-30% have cardiac manifestations (8). The most severe cardiopulmonary complication of mixed CTD is PAH, which results in increased RV pressure and has a fatal outcome in approximately half of patients (9). These late-stage phenomena, including endocarditis, atherosclerosis and pericarditis, may eventually lead to death or right heart failure in patients with CTD (10). Therefore, the detection of early-stage markers rather than late-stage markers in CTD development is a critical issue. RV abnormalities are associated with a risk of heart failure and cardiovascular death (11). RV dilatation and RV hypertrophy (RVH) are frequently observed in patients with CTD (12,13). Clinical evidence has shown that the RV structure can deteriorate despite a reduction in pulmonary vascular resistance after PAH-targeted therapies (14). RVH progression persists even when CTD-associated PAH is alleviated (15). This finding suggests that PAH may not be the sole indicator of RVH.

Cardiovascular magnetic resonance (CMR) can depict myocardial structure and characteristics using cine and late gadolinium enhancement (LGE) sequences, T1 mapping, and T1-derived ventricular extracellular volume (ECV) estimation (16). T1-mapping can be used to homogenously detect diffuse cardiac impairment (17) and predict the prognostic significance of CTD (18). Tissue tracking, a post processing method for strain analysis based on cine images from CMR, has been employed to assess the nature and function of myocardial tissue deformation (19).

Few studies have focused on cardiac involvement in patients with CTD (20) and fewer have focused on early detection of cardiac impairment (21). The present study explored factors that may predict the presence of RVH to reduce major adverse cardiovascular events in patients with CTD. Using clinical assessments and multi-imaging tests, the present study aimed to identify markers for the early detection of cardiac involvement preceding RVH.

Materials and methods

Study participants. All participants provided written informed consent and the study protocol was approved by the Institutional Review Boards of the Renji Hospital [approval no. (2017)083; Shanghai, China]. Consecutive participants, including patients with CTD without RVH, patients with CTD with RVH and control subjects, were prospectively enrolled in the three cohorts at Renji Hospital (Shanghai, China) between September 2017 and July 2018. The age range of patients in the control, non-RVH and RVH groups was 24-54, 23-57 and 30-54 years, respectively. The diagnosis of CTD was based on the clinical classification criteria, laboratory findings and imaging data (22). The inclusion criteria for patients with non-right ventricular hypertrophy (non-RVH) were as follows: i) Consecutive patients who presented to the outpatient clinic with SLE, polymyositis, systemic scleroderma, Sjögren's syndrome or mixed CTD diagnosis; ii) participants with CTD whose RV wall thickness was ≤4 mm were assigned to the non-RVH group according to echocardiography; iii) SLE duration was >6 months irrespective of cardiac symptoms. SLE activity and disease severity did not affect enrolment in the study; and iv) participants with RVH with an RV wall thickness >4 mm diagnosed using echocardiography (23). Age-matched candidates served as healthy controls and were used to establish the baseline myocardial T1 and strain values. Healthy volunteers with normal echocardiographic results and CMR findings were used as controls. The exclusion criteria were as follows: i) Age <18 or >80 years; ii) documented coronary artery disease and prior angiography for coronary artery disease (>50% stenosis); iii) patients with known congenital heart disease or other systemic diseases-induced RVH, including coronary artery disease, chronic obstructive pulmonary disease, primary pulmonary hypertension and valve disease; and iv) patients with standard metallic contraindications to CMR or an estimated glomerular filtration rate of <30 ml/min/1.73 m^2 and severe infection were excluded due to the consideration of CMR safety.

Clinical symptom assessment of patients with CTD. Clinical cardiac involvement of patients with CTD included clinical symptoms such as chest tightness, pectoralgia, heart palpitations, orthopnea, shortness of breath and edema. No specific myocardial enzymes were measured, and patients with CTD that may coexist with coronary artery disease, myocarditis, pericarditis, valvular heart disease, heart failure and PAH were not included in the present cohort study. The etiology of CTD and drug use were recorded.

ECG and RHC assessment. CTD-induced PAH was defined as an increase in mean pulmonary arterial pressure (PAP) of ≥20 mmHg at rest, as assessed by RHC (24). Within 48 h, pulmonary pressure was double-checked by echocardiography (E9; GE Healthcare). A CMR scan was scheduled within 6 h of echocardiography.

Follow-up. Telephone or outpatient consultations were used for the follow-up of the patients who survived every 3 months. When a patient died, cardiac death was identified from the death certificate. The shortest follow-up duration was >8 months.

CMR protocol. All CMR examinations were performed using a Philips 3T Ingenia MR system (Philips Healthcare).

Biventricular function. RV and LV volumetric assessments were obtained using cine imaging with whole-heart coverage of short-axis slices (7 mm thick with a 3-mm gap). Additionally, three long-axis views of the LV (4-, 2- and 3-chamber views) and two long-axis views of the RV (2- and 3-chamber views) were acquired. Detailed sequences and parameter settings are shown in Data S1.

Native and post-contrast T1 mapping. Native and post-contrast myocardial T1 mapping was used for ECV determination. A MOLLI R5.1 sequence was used for T1 mapping, and a '5-3-3' scheme (in sec) was chosen (details are presented in Data S1). The scheme was performed on three mid-diastolic LV short-axis slices (basal, mid-ventricle and apex) before and 15 min after a bolus intravenous injection of 0.15 mmol/kg gadobutrol (Bayer AG). Typical acquisition parameters are presented in Data S1.

Evaluation of LGE. LGE imaging was performed with no slice gap and whole heart coverage of short-axis slices 10 min after gadobutrol administration. Segmented LGE images

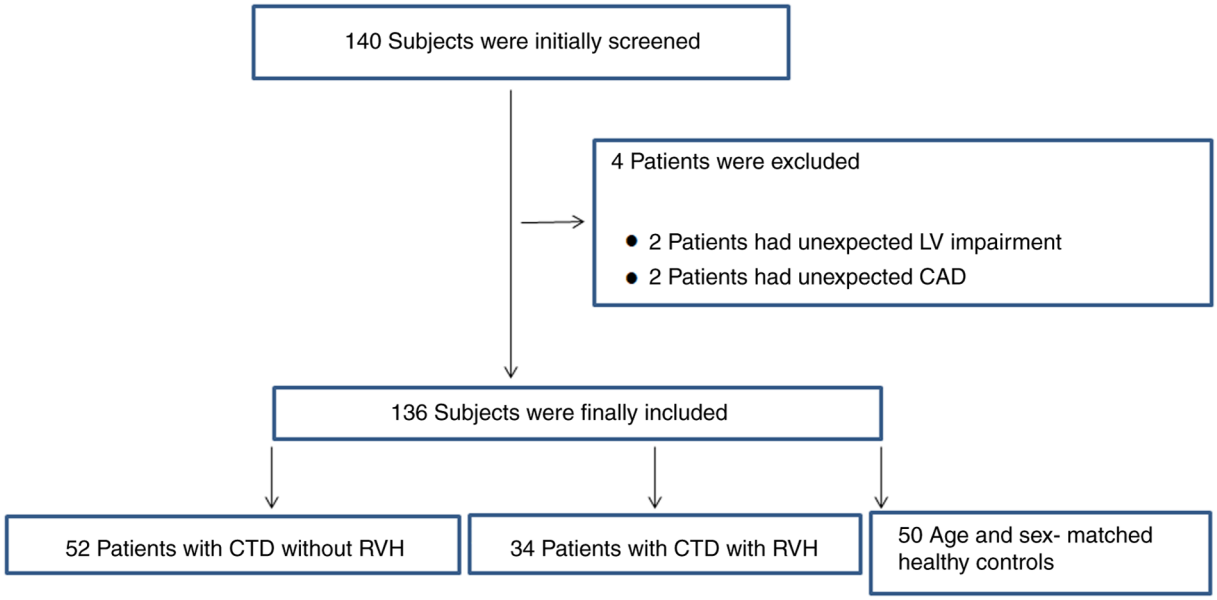

Figure 1. Flow chart of the present study. The diagram shows participants in the screening. CAD, coronary artery disease; CTD, connective tissue disease; LV, left ventricle; RVH, right ventricular hypertrophy.

with at least three matching slices and native T1 images were obtained. A visual assessment of LGE positivity was performed. The acquisition parameters are shown in Data S1.

Cardiac image analysis: Bi-ventricular morphology, function and myocardial deformation. LV and RV function parameters, mass, volume, ejection fractions, and strain were assessed using Circle (cvi42 version 5.5.6.1; Circle Cardiovascular Imaging, Inc.). CMR data analysis was performed by two observers who are experienced in CMR and were blinded to the clinical information. For the LV and RV volumes and masses, the endocardial borders were manually traced at end-diastole and end-systole. The papillary muscles were included as part of the myocardium. All volumetric indices were normalized to body surface area (BSA). An RV/LV volume ratio >1.27 was defined as RV enlargement (25). An RV wall thickness >4 mm indicates RVH and RV pressure overload in the absence of other explanatory pathologies (23).

The LV and RV global circumferential strain and global radial strain were obtained in the short-axis view at the apical, midventricular and basal levels, and the global longitudinal strain was derived from the long-axis view (2-, 3- and 4-chamber images). Myocardial deformation was voxel-tracked, and software-integrated contours automatically tracked distinctive features within a user-defined region of interest throughout the cardiac cycle. All contours were manually examined, adjusted when necessary, and assessed.

Fibrosis assessment: LGE, ECV quantification and quality assessment. LGE, T1 and ECV images were used to examine the presence and extent of regional and diffuse fibrosis (cvi42 version 5.5.6.1). The methods for creating parametric maps and quality assessments are provided in Data S1. The reported T1 values were derived by an operator blinded to the LGE images. Hematocrit was measured on the same day for all participants. The ECV was calculated using the ECV formula: ECV=1-hematocrit x (1/T1 myo post-1/T1 myo pre)/(1/T1 blood post/1/T1 blood pre). T1 and ECV quantification details are provided in Data S1.

Statistical analysis. Quantitative data are presented as the mean ± SD or the median (interquartile range), and categorical data are presented as numbers and percentages. Quantitative data were checked for normality using the Kolmogorov-Smirnov test, and the three groups were compared using one-way analysis of variance and post hoc Bonferroni correction. The Kruskal-Wallis test and post hoc Bonferroni test were used for among-group comparisons. For categorical data, comparisons among the three groups were performed using Pearson's χ^2 test or Fisher's exact test. Furthermore, a second blinded operator calculated >50% of the randomly selected cases. The same analysis technique was used, and the inter-observer reproducibility of volume, strain, T1 mapping and ECV measurements was assessed using intra-class correlation coefficient analysis. Univariate and multivariate regression analyses of RV myocardial infarction (RVMI) outcomes were performed to identify statistically significant determinants. All analyses were performed using IBM SPSS Statistics software (version 17.0; SPSS, Inc.). $P<0.05$ (two-tailed) was considered to indicate a statistically significant difference.

Results

Screening of enrolled patients. A total of 140 participants were recruited based on the inclusion and exclusion criteria. A total of 4 patients were excluded: 2 patients had unexpected LV impairment and 2 patients had unexpected coronary artery disease. Consequently, 136 patients were recruited, including 52 patients without RVH, 34 patients with RVH and 50 age-matched healthy controls. The final patient selection flowchart is shown in Fig. 1.

Table I. Inter-observer agreement for strain, volume and T1 values.

Variables	ICC (95% CI)	F statistic	P-value
Strains			
Global radial strain (%)			
Left ventricle	0.924 (0.841-0.964)	14.207	<0.001
Right ventricle	0.856 (0.697-0.931)	0.528	<0.001
Global circumferential strain (%)			
Left ventricle	0.955 (0.905-0.979)	66.683	<0.001
Right ventricle	0.899 (0.787-0.952)	4.637	<0.001
Global longitudinal strain (%)			
Left ventricle	0.895 (0.780-0.950)	66.495	<0.001
Right ventricle	0.588 (0.135-0.804)	0.141	0.010
Biventricular morphology and function			
Right ventricle			
RVEF	0.984 (0.967-0.992)	2.163	<0.001
RVEDV/BSA	0.997 (0.994-0.999)	2.592	<0.001
RVESV/BSA	0.994 (0.987-0.997)	0.319	<0.001
Left ventricle			
LVEF	0.987 (0.973-0.994)	0.982	<0.001
LVEDV/BSA	0.972 (0.941-0.987)	3.526	<0.001
LVESV/BSA	0.991 (0.981-0.996)	0.036	<0.001
RVEDV/LVEDV	0.813 (0.608-0.911)	1.207	<0.001
T1 values and ECV			
Left ventricle			
Native T1 myo	0.981 (0.958-0.991)	39.083	<0.001
T1-post myo	0.993 (0.986-0.997)	9.057	<0.001
ECV	0.958 (0.909-0.981)	13.837	<0.001
Right ventricle			
Native T1 myo	0.930 (0.781-0.977)	0.002	<0.001
T1-post myo	0.919 (0.749-0.974)	0.864	<0.001
ECV	0.758 (0.246-0.922)	3.163	0.008

ICC, intraclass correlation coefficient; BSA, body surface area; RVEF, right ventricular ejection fraction; RVEDV, right ventricular end diastolic volume; RVESV, right ventricular end systolic volume; LVEF, left ventricular ejection fraction; LVEDV, left ventricular end diastolic volume; LVESV, left ventricular end systolic volume; ECV, ventricular extracellular volume; myo, myocardial tissue.

Inter-observer assessment of reproducibility. Table I summarizes the inter-observer variability in biventricular volumes, strain and T1 values. Intraclass correlation coefficient analysis indicated a strong association, except for the global longitudinal strain of the right ventricle, between the two operators.

Characteristics of patients. The baseline characteristics of the patients are summarized in Table II. Sex and BSA were comparable between the two diseased groups, consisting primarily of female patients with significantly lower BSA levels than those of the control group (P<0.05). The etiologies were comparable between the non-RVH and RVH groups (P>0.05). More patients with RVH tended to receive endothelial receptor antagonists and prostacyclin medications than those in the non-RVH group (P<0.05). Both diseased groups had accelerated heartbeats compared with the control group (P<0.001). Except for heart rate, the non-RVH and RVH groups also had high brain natriuretic peptide (P<0.001), troponin I (P<0.001) and creatine kinase-MB (P=0.004) levels, but low creatine phosphate kinase levels (P<0.001) compared with the control group. In addition, according to the ECG results, in the non-RVH and RVH groups, the incidence (30/34; 88%) and values (76±23 mmHg) of pulmonary hypertension in the RVH group were significantly increased compared with those in the control group (0/50; 0% incidence and 22±21 mmHg; P<0.001) (Table II).

Cardiac systolic function and dimensions. Notably, more RV parameters were affected than LV parameters (Table II). RVH was associated and significantly increased with RV dilatation in terms of RV end-diastolic volume (RVEDV), RV end-systolic volume (RVESV), RVEDV/BSA and RVESV/BSA indices (P=0.016) compared with those of the control group. The chamber dilatation led to a reduction in RV ejection fraction (RVEF) (40±11% in the RVH group vs. 55±10% in the non-RVH group and 62±9% in the control group for RVEF, P<0.001; 63±12% in the RVH group vs. 63±12% in

Table II. Baseline characteristics.

Characteristics	Controls (n=50)	Non-RVH (n=52)	RVH (n=34)	P-value[a]
Clinical				
Age, years	39±15	35±12	42±12[b]	0.450
Female, n (%)	30 (60)	46 (88)[c]	32 (94)[c]	<0.001
BSA, m^2	1.76±0.21	1.56±0.17[c]	1.58±0.18[c]	<0.001
Vital signs				
Heart rate, bpm	72±13	78±14[c]	83±13[c]	0.001
Systolic BP, mmHg	123±18	119±16	118±19	0.360
Diastolic BP, mmHg	78±12	75±12	78±13	0.554
Serum markers of cardiac injury				
BNP, pg/ml	52 (26, 167)	89 (39, 291)[c]	358 (62, 784)[c]	<0.001
TNI, ng/ml	0.00 (0.00, 0.01)	0.01 (0.01, 0.05)[c]	0.01 (0.01, 0.03)[c]	<0.001
CPK, U/l	99 (72, 134)	50 (27, 148)[c]	50 (34, 107)[c]	<0.001
CK-MB, ng/ml	1.50 (1.20, 2.20)	8.00 (0.70, 19.50)[c]	5.25 (2.80, 11.70)[c]	0.004
ACC/AHA stages C-D, n (%)	0 (0)	2 (4)	5 (15)	0.160
ECG abnormal, n (%)	0 (0)	26 (50)	25 (74)[b]	0.030
Pulmonary hypertension, n (%)	0 (0)	24 (46)	30 (88)[b]	<0.001
PAH, mmHg	22±21	31±21	76±23[b,c]	<0.001
Etiology				
Systemic lupus erythematosus, n (%)	0 (0)	40 (76)	19 (56)	0.070
Polymyositis, n (%)	0 (0)	6 (12)	1 (3)	0.300
Systemic scleroderma, n (%)	0 (0)	2 (4)	2 (6)	0.930
Sjogren syndrome, n (%)	0 (0)	1 (2)	3 (9)	0.330
Mixed connective tissue disease, n (%)	0 (0)	3 (6)	9 (27)	0.080
Medical therapy				
None, n (%)	50 (100)	41 (79)[c]	13 (38)[b,c]	<0.001
Calcium antagonists, n (%)	0 (0)	4 (8)	3 (9)	0.850
Endothelial receptor antagonists, n (%)	0 (0)	1 (2)	13 (38)[b]	<0.001
Phosphodiesterase indicator, n (%)	0 (0)	1 (2)	5 (15)	0.060
Prostacyclin, n (%)	0 (0)	7 (13)	15 (44)[b]	0.001
CMR				
LV morphology and function				
LVEDV, ml	122±34	118±32	85±34[b,c]	<0.001
LVEDV/BSA, ml/m^2	69±15	76±22	54±18[b,c]	<0.001
LVESV, ml	41±15	45±26	34±24[b,c]	0.004
LVESV/BSA, ml/m^2	23±8	29±19	21±13[b]	0.016
LV mass, g	111±32	110±30	113±74	0.050
LV mass/BSA, g/m^2	62±13	71±21	71±46	<0.001
LVEF, %	67±7	63±12	63±12	0.171
RV morphology and function				
RVEDV, ml	107±32	112±31	145±45[b,c]	0.003
RVEDV/BSA, ml/m^2	60±14	73±20[c]	92±26[b,c]	<0.001
RVESV, ml	41±15	51±19[c]	89±37[b,c]	<0.001
RVESV/BSA, ml/m^2	23±8	33±12[c]	56±22[b,c]	<0.001
RV mass, g	32±12	34±8	57±21[b,c]	<0.001
RV mass/BSA, g/m^2	18±6	22±6[c]	36±12[b,c]	<0.001
RVEF, %	62±9	55±10[c]	40±11[b,c]	<0.001
RVESV/LVESV	0.87±0.10	0.98±0.26[c]	2.09±1.14[b,c]	<0.001
Myocardial fibrosis				
LGE size, %	0 (0)	0 (0, 0)	4.53 (2.32, 9.79)[b]	<0.001
LGE (+), n (%)	0 (0)	8 (15)	28 (82)[b]	<0.001
Death				
All-cause mortality, n (%)	0 (0)	3 (6)	2 (6)	0.200

Table II. Continued.

Characteristics	Controls (n=50)	Non-RVH (n=52)	RVH (n=34)	P-value[a]
Cardiac death, n (%)	0 (0)	2 (4)	1 (3)	0.140

[a]P-value across the three groups. [b]P<0.05 (RVH group vs. non-RVH group). [c]P<0.05 (individual group vs. controls). Values are presented as the mean ± SD, number (%) or median (25-75th percentile). ACC/AHA stages, American College of Cardiology/American Heart Association classification of heart failure stages; BP, blood pressure; BSA, body surface area; BNP, brain natriuretic peptide; TNI, troponin I; CK-MB, creatine kinase-MB; CPK, creatine phosphate kinase; ECG, electrocardiogram; PAH, pulmonary arterial hypertension; CMR, cardiovascular magnetic resonance; LV, left ventricle; LVEDV, left ventricular end diastolic volume; LVESV, left ventricular end systolic volume; LVEF, left ventricular ejection fraction; RV, right ventricle; RVEDV, right ventricular end diastolic volume; RVESV, right ventricular end systolic volume; RVEF, right ventricular ejection fraction; RVH, right ventricular hypertrophy; LGE, late gadolinium enhancement.

Table III. Native and post-contrast T1 relaxation times for the LV.

	LV			
Variables	Controls (n=50)	Non-RVH(n=52)	RVH (n=34)	P-value[a]
Native T1 myocardium, msec	1,268±42	1,362±72[b]	1,372±89[b]	<0.0001
Post (15 min) T1 myocardium, msec	613±39	661±66[b]	585±63[c]	<0.001
ECV, %	25±3	31±4[b]	32±5[b]	<0.001

[a]P-value across the three groups. [b]P<0.05 (individual group vs. controls). [c]P<0.05 (non-RVH group vs. RVH group). Values are presented as the mean ± SD. LV, left ventricle; ECV, ventricular extracellular volume; RVH, right ventricular hypertrophy.

the non-RVH group and 67±7% in the control group for the LVEF, P=0.171). In the non-RVH group, RV dimensions were normal [RV end systolic volume (RVESV)/LV end systolic volume, 0.98±0.26 in the non-RVH group vs. 0.87±0.1 in the control group; P=0.5], the RVEF was within the normal range (51-71%), and no LV morphological or functional impairment was observed.

Prevalence and extent of LV myocardial fibrosis in the non-RVH and RVH groups. LGE is a biomarker for regional myocardial fibrosis (26). In the non-RVH group, positive fibrosis [LGE (+)] was observed in 15.4% (8/52) of patients and the median LV extent (LGE size) was 0.0 (0,0 for 25-75% quartile). By contrast, the LGE(+) incidence in the RVH group was 82.4% (28/34) and the median LGE size was 4.53 (2.32-9.79 for 25-75% quartile) (Table II). The LGE(+) incidence and LGE size in the non-RVH group were significantly decreased compared with those in the RVH group. Table III summarizes the T1 and ECV values of the LV. Notably, the native LV myocardial T1 and ECV were increased in the non-RVH group (all P<0.001; compared with controls). The values were not significantly different between the non-RVH and RVH groups (native myocardial T1: 1,362±72 msec in the non-RVH group vs. 1,372±89 msec in the RVH group; P=0.61; ECV: 31±4% in the non-RVH group vs. 32±5% in the RVH group; P=0.24). Fig. 2 shows examples of regional and diffuse myocardial fibrosis in patients. Native myocardial T1 and ECV detected increased fibrosis through values and color maps, even when LGE was negative (second column; a patient with non-RVH).

Furthermore, the T1 values of the hypertrophied RV were investigated in the RVH group (Table IV). The hypertrophied RV free wall exhibited significantly increased native T1 (1,463±130 msec) and ECV (37±6%) levels compared with the septum with LGE(+) (1,392±96) and ECV (34±5) (P<0.001 for myocardial native T1; P=0.108 for ECV). By contrast, T1 myocardium 15 min post-contrast T1 relaxation did not significantly differ between the hypertrophied RV free wall (576±70) and the septum with LGE(+) (560±69) (P=0.222 for post T1).

Biventricular myocardial deformation. The global myocardial deformation is shown in Fig. 3. Global longitudinal and circumferential strains of the RVH group were significantly increased compared with those in the control group (P<0.01). Global circumferential strain in the RVH groups was not significantly increased compared with that in the non-RVH group (P=0.19). However, global radial strain in the RVH group was markedly lower than that in the control (P<0.01) and non-RVH groups (P=0.01) (Fig. 3A). In the LV, LV global longitudinal strain was the only index with strain reduction in the non-RVH and RVH groups (-14.82±2.6 msec in the control group; -13.23±3.22 msec in the non-RVH group; -12.82±3.93 msec in the RVH group; P=0.03 for the non-RVH group and P=0.01 for the RVH group compared with the control group). The global radial and circumferential strains of the LV were not markedly reduced in the non-RVH or RVH groups compared with those in the control group (Fig. 3B). Examples of the RV and LV mean global longitudinal strain in the three groups of patients are shown in Fig. 4 to demonstrate the same results individually. The curves in Fig. 4 were representative and randomly selected, showing data from 1 patient in each group.

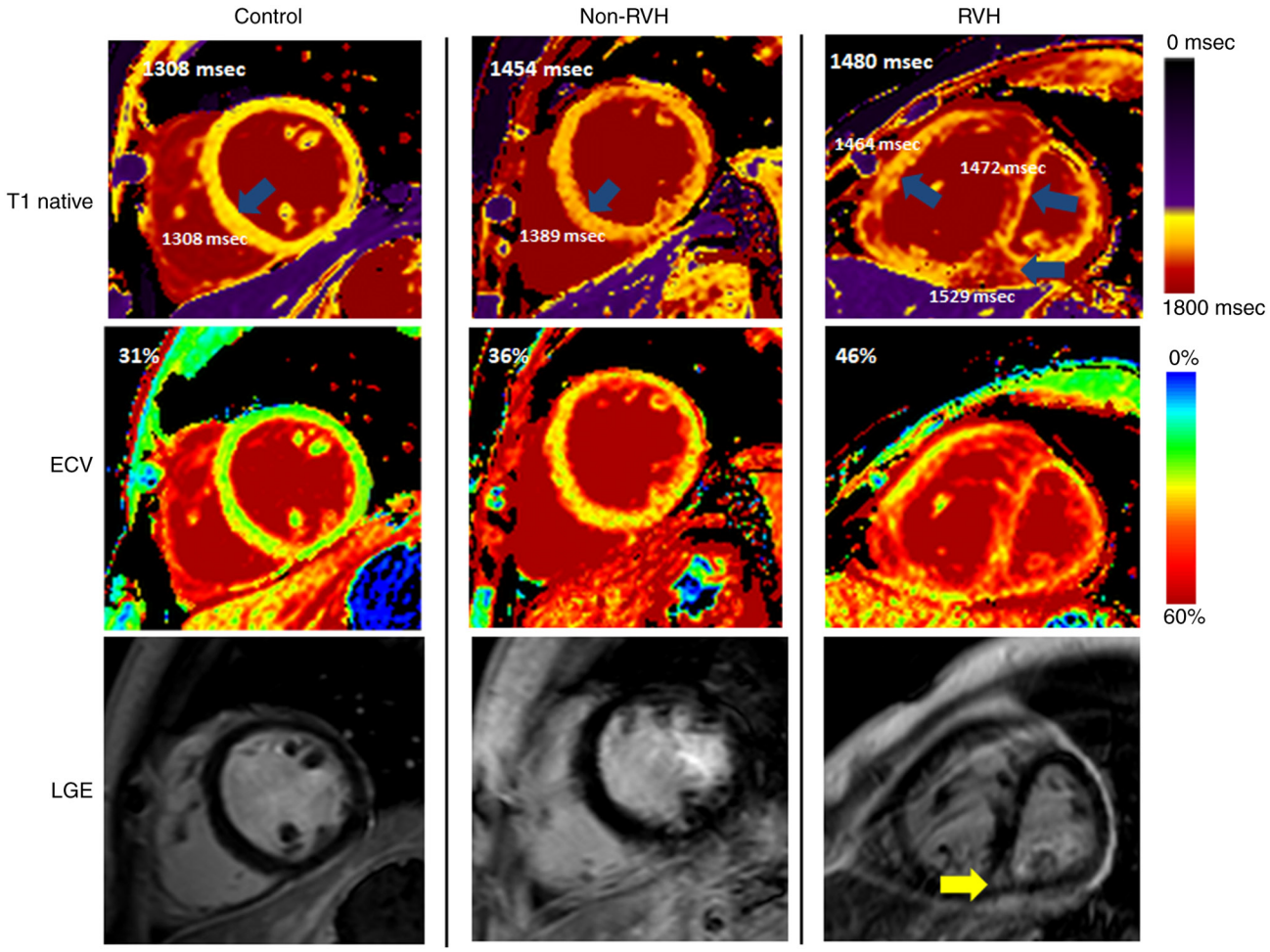

Figure 2. Example of regional and diffuse fibrosis distribution in patients in the non-RVH and RVH groups. Native myocardial T1 values and ECV are presented as values and a color map to show the increased fibrotic features in patients with non-RVH and RVH. Unlike the positive foci seen in patients with RVH (yellow arrow), there was no visual regional fibrosis present (blue arrows) in the patients with non-RVH. ECV, ventricular extracellular volume; LGE, late gadolinium enhancement; RVH, right ventricular hypertrophy.

Predictors of increases in the RV mass index. Regarding the predictors of an increase in the RV mass index, all baseline clinical and CMR parameters in Tables I and II were included in the univariate regression analysis with RVMI outcomes (Table V). Parameters selected via the univariate analysis ($P<0.05$) were included in a multivariate regression analysis, which demonstrated that PAP predicted RVH when the RV wall thickness was within the normal range ($P=0.01$). In the group with RVH, RV end-systolic volume was a predictor of RVH ($P<0.0001$). No other cardiac imaging or laboratory findings were predictors of RVH.

Prognosis of the non-RVH and RVH groups. The mean duration of follow-up was 12.1±4.5 and 10.8±3.5 months for the non-RVH and RVH groups, respectively. Notably, 2 of 52 patients (4%) in the non-RVH group and 1 of 34 patients in the RVH group (3%) died due to cardiac death during follow-up. The death rates were similar ($P=0.14$; Table II).

Discussion

The major findings of the present study were as follows: i) Patients with RVH had impaired RVEF, RV dimensions and global longitudinal strain compared with the non-RVH and control groups; ii) fibrosis assessment by CMR revealed that native T1 values and the ECV in patients in the RVH and non-RVH groups were significantly higher than those in the control group; and iii) PAP in the non-RVH stage and RVESV in the RVH stage predicted RVH progression.

A previous study has suggested that PAH may not be the sole predictor of progressive RV failure and death in patients with CTD (27). To further understand other predictors of RV failure, we hypothesized that the predictors would vary with the disease stage of the target organs. In the non-RVH stage, RVH is primarily driven by PAH (pressure overload), which induces an increase in the RV pressure that, without timely intervention, may progress into compensatory RVH. Late-stage phenomena, such as prominent RV dilatation, were not observed in the non-RVH stage (2,28), possibly suggesting that treatment intervention at this time might contribute to preventing or reversing further damage to the myocardium.

Once a patient enters the RVH stage, progressive right-sided heart failure or sudden and unexpected death can occur, and simple cardiac protection may not be beneficial because of the damage to the cardiac tissue substrate and its structure and function (29,30). Extensively increased biventricular

Table IV. Right ventricular native and post-contrast T1 relaxation times in the right ventricular hypertrophy group (n=34).

Variables	Septum with LGE (+)	Septum without LGE (+)	Right ventricular free wall	P-value[a]
NativeT1 myocardium, msec	1,392±96	1,357±93	1,463±130[b,c]	<0.001
Post (15 min) T1 myocardium, msec	560±69	568±66	576±70	0.222
ECV, %	34±5	33±4	37±6	0.108

[a]P-value across the three groups. [b]P<0.05 [RV myocardium vs. septum with LGE (+)]. [c]P<0.05 [RV myocardium vs. septum without LGE (+)]. Values are presented as the mean ± SD. ECV, ventricular extracellular volume; LGE, late gadolinium enhancement; RV, right ventricle.

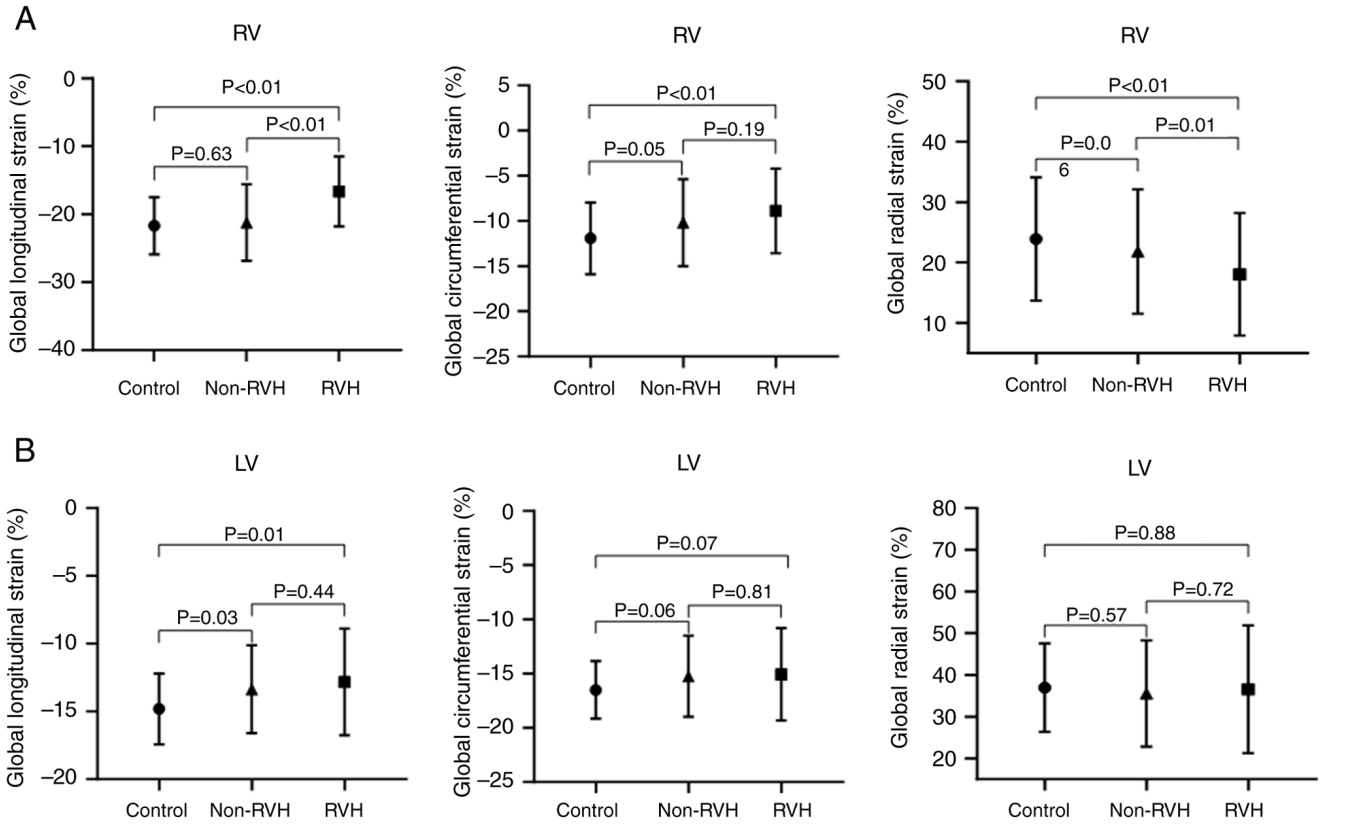

Figure 3. Global strains in patients with non-RVH and RVH. (A) Global strain in the RV. (B) Global strain in the LV. Global longitudinal, circumferential and radial strains are shown from left to right. LV, left ventricle; RV, right ventricle; RVH, right ventricular hypertrophy.

extracellular matrix and regional LGE accounted for the reduced RV strain and the lack of RV contraction, which led to an increase in RVESV. Therefore, the RVESV became a predictor of RVH progression.

The present study primarily focused on the early detection of myocardial damage. Pulmonary pressure measurements from routine echocardiographic examinations are both practical and important because routine echocardiographic examination can be used for guidance of patient treatments. For example, once PAH was detected, 88% of patients in the RVH group had PAH, which increased to 76±23 (mean ± SD). In addition, the right heart structural and functional abnormality appeared. Although PAH can guide treatment, it is often delayed (31). Therefore, early indicators that identify the presence of myocardial damage, which are the focus of the present study, are urgently needed.

Concerning all clinical and imaging parameters, only native T1 values, T1-deduced ECV and longitudinal strain can be used to screen for myocardial abnormalities in the non-RVH stage (26). The first two parameters represent the extracellular matrix, which indirectly reflects diffuse fibrotic changes (32,33), whereas the last parameter indicates myocardial deformation, which may be due to LV chamber compression caused by RV dilatation (34). Furthermore, native T1, ECV and longitudinal strain are warning signs of heart involvement in patients with a normal cardiac systolic ejection fraction (35). Theoretically, a histological increase in myocardial fibrosis may occur first, followed by a decrease in myocardial deformation; ventricular structural and functional abnormalities may occur later (36). Notably, whether CTD treatment is effective in reversing cardiac damage remains unclear.

Table V. Predictors of an increase in the right ventricular mass index.

Groups	Predictors	Univariate analysis				Multivariate analysis			
		Coefficient	SE	t-statistic	P-value	Coefficient	SE	t-statistic	P-value
Non-RVH	RVESV	0.12	0.05	2.20	0.03	-0.21	0.17	-1.25	0.22
	RVESV/BSA	0.21	0.08	2.82	0.01	0.04	0.08	0.44	0.66
	RVEDV/BSA	0.13	0.05	2.83	0.01	0.37	0.28	1.32	0.19
	LVEDV/BSA	11.52	4.12	2.80	0.01	0.03	0.05	1.32	0.19
	PAP	7.32	0.43	16.87	0.01	0.16	0.06	2.84	0.01
RVH	RVESV	0.23	0.03	7.98	<0.0001	0.23	0.03	7.98	<0.0001
	RVESV/BSA	0.37	0.05	7.90	<0.0001	-0.4	1.29	-0.31	0.49
	RVEDV	0.15	0.03	5.92	<0.0001	-0.29	0.53	-0.55	0.59
	RVEDV/BSA	0.26	0.04	5.79	<0.0001	0.31	0.78	0.39	0.69
	RVEDV/RVESV	7.33	1.38	5.31	<0.0001	0.11	3.09	0.03	0.97
	RVEF	-0.57	0.15	-3.79	0.01	0.14	0.36	0.38	0.71
	LV cardiac output/BSA	-6.68	2.73	-2.45	0.02	-1.31	3.09	-0.42	0.67
	LV stroke volume/BSA	-0.61	0.21	-2.91	0.01	-0.03	0.33	-0.08	0.93

BSA, body surface area; PAP, pulmonary arterial pressure; LV, left ventricle; LVEDV, left ventricular end diastolic volume; RVEDV, right ventricular end diastolic volume; RVESV, right ventricular end systolic volume; RVEF, right ventricular ejection fraction; RVH, right ventricular hypertrophy; SE, standard error.

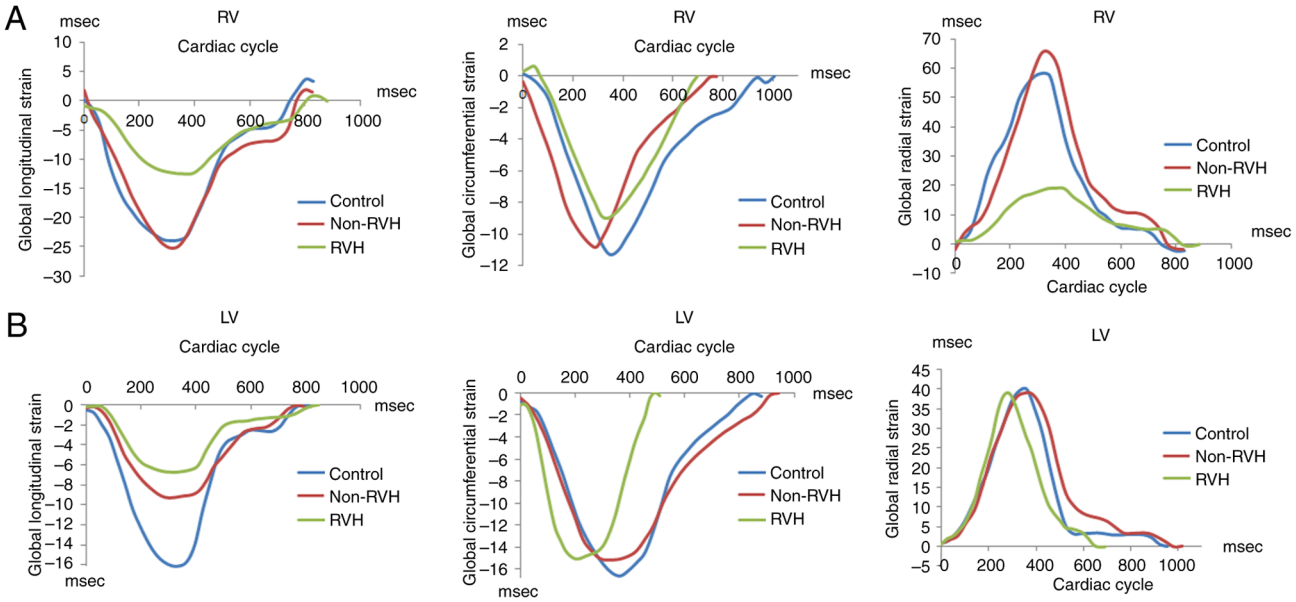

Figure 4. Examples of global strain in patients with non-RVH and RVH. (A) Three examples from representative patients showing RV strain in longitudinal, circumferential and radial directions. The strain in each direction was decreased in patients with RVH (green line). Patients with non-RVH had no reduced strain in either direction. (B) In the left ventricle, global longitudinal strain in patients with non-RVH (red line) and RVH (green line) was reduced compared with that in control subjects (left panel). No strain reduction was observed among patients in terms of the circumferential and radial strains. LV, left ventricle; RV, right ventricle; RVH, right ventricular hypertrophy.

Non-invasive detection of cardiac tissue characterization may become a recommendation in the future, as it favors the early detection of cardiac impairment. Furthermore, PAH was not the sole predictor of progressive RV failure or death in patients with CTD. The predictors varied according to the presence of RVH. Finally, native myocardial T1, ECV and LV longitudinal strains can be used as warning signs of myocardial damage in patients with CTD.

The present study had some limitations. First, mixed etiologies of CTD, which may complicate cardiac pathophysiological mechanisms, were included in the present study. However, the varied etiologies were equally distributed between the groups, which eliminated the difference. Second, caution should be exercised regarding mortality rates. The relatively short follow-up period and low mortality rate make the results prone to bias. Third, the sample size of the present study was small,

which may have resulted in sample bias. Forth, all patients were from one medical center, which may give rise to selection bias. Finally, the present cross-sectional study proposed markers of myocardial impairment; however, whether they can serve as follow-up indicators and their mechanisms require further evaluation. To overcome these limitations, the sample size will be expanded and data from multiple medical centers will be combined in the future. Future studies will also focus on detecting RV contractility in PAH, compensated heart failure and decompensated heart failure periods of RVH. These results will reveal more detailed mechanisms of myocardial damage in patients with CTD.

In conclusion, non-invasive examination of cardiac tissue characterization using CMR enabled the early detection of cardiac impairment before RVH development. Native myocardial T1, ECV and LV longitudinal strain may serve as warning signs of myocardial damage in patients with CTD. The predictors of RVH varied with heart disease stages. PAP in the non-RVH stage and RVESV in the RVH stage predicted further RVH progression.

Acknowledgements

Not applicable.

Funding

The present study was supported by the National Science Foundation of China (grant no. 81470391), Shanghai Municipal Education Commission-Gaofeng Clinical Medicine Grant Support (grant no. 20172014), and a three-year action plan to promote clinical skills and clinical innovation in municipal hospitals (grant no. 16CR3020A).

Availability of data and materials

The data generated in the present study may be requested from the corresponding author.

Authors' contributions

JS, MJ and SZ were responsible for the conception and design of the study. JS, GX, SF, HY, ZZ and YX were responsible for acquisition and analysis of the data. MJ and SZ confirmed the authenticity of all the raw data. MJ was the main supervisor and SZ was the co-supervisor. JS, MJ and SZ wrote the manuscript. All authors read and approved the final manuscript.

Ethics approval and consent to participate

The present study was reviewed and approved by the Institutional Review Boards of the Renji Hospital, Shanghai Jiaotong University [approval no. (2017)083; Shanghai, China]. All participants provided written informed consent for participation.

Patient consent for publication

Written informed consent for publication was obtained from all individual participants included in the study.

Competing interests

The authors declare that they have no competing interests.

References

1. Braun J, Krüger K, Manger B, Schneider M, Specker C and Trappe HJ: Cardiovascular comorbidity in inflammatory rheumatological conditions. Dtsch Arztebl Int 114: 197-203, 2017.
2. Dawi J, Affa S, Misakyan Y, Fardeheb S, Kades S, Kiriaki A, Mohan AS, Norris B, Yoon S and Venketaraman V: Exploring cardiovascular implications in systemic lupus erythematosus: A holistic analysis of complications, diagnostic criteria, and therapeutic modalities, encompassing pharmacological and adjuvant approaches. Biomol Concepts 15, 2024.
3. Miner JJ and Kim AH: Cardiac manifestations of systemic lupus erythematosus. Rheum Dis Clin North Am 40: 51-60, 2014.
4. Schermuly RT, Ghofrani HA, Wilkins MR and Grimminger F: Mechanisms of disease: Pulmonary arterial hypertension. Nat Rev Cardiol 8: 443-455, 2011.
5. Wigley FM, Lima JAC, Mayes M, McLain D, Chapin JL and Ward-Able C: The prevalence of undiagnosed pulmonary arterial hypertension in subjects with connective tissue disease at the secondary health care level of community-based rheumatologists (the UNCOVER study). Arthritis Rheum 52: 2125-2132, 2005.
6. Plazak W, Gryga K, Milewski M, Podolec M, Kostkiewicz M, Podolec P and Musial J: Association of heart structure and function abnormalities with laboratory findings in patients with systemic lupus erythematosus. Lupus 20: 936-944, 2011.
7. Hassoun PM: The right ventricle in scleroderma (2013 grover conference series). Pulm Circ 5: 3-14, 2015.
8. Alpert MA, Goldberg SH, Singsen BH, Durham JB, Sharp GC, Ahmad M, Madigan NP, Hurst DP and Sullivan WD: Cardiovascular manifestations of mixed connective tissue disease in adults. Circulation 68: 1182-1193, 1983.
9. Vegh J, Hegedus I, Szegedi G, Zeher M and Bodolay E: Diastolic function of the heart in mixed connective tissue disease. Clin Rheumatol 26: 176-181, 2007.
10. Leal GN, Silva KF, França CMP, Lianza AC, Andrade JL, Campos LMA, Bonfá E and Silva CA: Subclinical right ventricle systolic dysfunction in childhood-onset systemic lupus erythematosus: Insights from two-dimensional speckle-tracking echocardiography. Lupus 24: 613-620, 2015.
11. Kawut SM, Barr RG, Lima JAC, Praestgaard A, Johnson WC, Chahal H, Ogunyankin KO, Bristow MR, Kizer JR, Tandri H and Bluemke DA: Right ventricular structure is associated with the risk of heart failure and cardiovascular death: The Multi-Ethnic Study of Atherosclerosis (MESA)-right ventricle study. Circulation 126: 1681-1688, 2012.
12. Tang Y, Yang Z, Wen J, Tang D, Luo Y, Xiang C, Huang L and Xia L: Association of serum uric acid with right cardiac chamber remodeling assessed by cardiovascular magnetic resonance feature tracking in patients with connective tissue disease. Front Endocrinol (Lausanne) 15: 1351197, 2024.
13. Vos JL, Butcher SC, Fortuni F, Galloo X, Rodwell L, Vonk MC, Bax JJ, van Leuven SI, de Vries-Bouwstra JK, Snoeren M, *et al*: The prognostic value of right atrial and right ventricular functional parameters in systemic sclerosis. Front Cardiovasc Med 9: 845359, 2022.
14. Rich S, Pogoriler J, Husain AN, Toth PT, Gomberg-Maitland M and Archer SL: Long-term effects of epoprostenol on the pulmonary vasculature in idiopathic pulmonary arterial hypertension. Chest 138: 1234-1239, 2010.
15. Bell RD, White RJ, Garcia-Hernandez ML, Wu E, Rahimi H, Marangoni RG, Slattery P, Duemmel S, Nuzzo M, Huertas N, *et al*: Tumor necrosis factor induces obliterative pulmonary vascular disease in a novel model of connective tissue disease-associated pulmonary arterial hypertension. Arthritis Rheumatol 72: 1759-1770, 2020.
16. Messroghli DR, Moon JC, Ferreira VM, Grosse-Wortmann L, He T, Kellman P, Mascherbauer J, Nezafat R, Salerno M, Schelbert EB, *et al*: Clinical recommendations for cardiovascular magnetic resonance mapping of T1, T2, T2* and extracellular volume: A consensus statement by the society for cardiovascular magnetic resonance (SCMR) endorsed by the European association for cardiovascular imaging (EACVI). J Cardiovasc Magn Reson 19: 75, 2017.

17. White SK, Sado DM, Flett AS and Moon JC: Characterising the myocardial interstitial space: The clinical relevance of non-invasive imaging. Heart 98: 773-779, 2012.
18. Wong TC, Piehler KM, Kang IA, Kadakkal A, Kellman P, Schwartzman DS, Mulukutla SR, Simon MA, Shroff SG, Kuller LH and Schelbert EB: Myocardial extracellular volume fraction quantified by cardiovascular magnetic resonance is increased in diabetes and associated with mortality and incident heart failure admission. Eur Heart J 35: 657-664, 2014.
19. Broberg CS, Chugh SS, Conklin C, Sahn DJ and Jerosch-Herold M: Quantification of diffuse myocardial fibrosis and its association with myocardial dysfunction in congenital heart disease. Circ Cardiovasc Imaging 3: 727-734, 2010.
20. Hachulla AL, Launay D, Gaxotte V, de Groote P, Lamblin N, Devos P, Hatron PY, Beregi JP and Hachulla E: Cardiac magnetic resonance imaging in systemic sclerosis: A cross-sectional observational study of 52 patients. Ann Rheum Dis 68: 1878-1884, 2009.
21. Mavrogeni S, Sfikakis PP, Karabela G, Stavropoulos E, Spiliotis G, Gialafos E, Panopoulos S, Bournia V, Manolopoulou D, Kolovou G and Kitas G: Cardiovascular magnetic resonance imaging in asymptomatic patients with connective tissue disease and recent onset left bundle branch block. Int J Cardiol 171: 82-87, 2014.
22. Zhernakova A, van Diemen CC and Wijmenga C: Detecting shared pathogenesis from the shared genetics of immune-related diseases. Nat Rev Genet 10: 43-55, 2009.
23. Rudski LG, Lai WW, Afilalo J, Hua L, Handschumacher MD, Chandrasekaran K, Solomon SD, Louie EK and Schiller NB: Guidelines for the echocardiographic assessment of the right heart in adults: A report from the American society of echocardiography endorsed by the European association of echocardiography, a registered branch of the European society of cardiology, and the canadian society of echocardiography. J Am Soc Echocardiogr 23: 685-713, 786-788, 2010.
24. Humbert M, Kovacs G, Hoeper MM, Badagliacca R, Berger RMF, Brida M, Carlsen J, Coats AJS, Escribano-Subias P, Ferrari P, *et al*: 2022 ESC/ERS guidelines for the diagnosis and treatment of pulmonary hypertension. Eur Heart J 43: 3618-3731, 2022.
25. Altmayer SPL, Patel AR, Addetia K, Gomberg-Maitland M, Forfia PR and Han Y: Cardiac MRI right ventricle/left ventricle (RV/LV) volume ratio improves detection of RV enlargement. J Magn Reson Imaging 43: 1379-1385, 2016.
26. Minegishi S, Kato S, Takase-Minegishi K, Horita N, Azushima K, Wakui H, Ishigami T, Kosuge M, Kimura K and Tamura K: Native T1 time and extracellular volume fraction in differentiation of normal myocardium from non-ischemic dilated and hypertrophic cardiomyopathy myocardium: A systematic review and meta-analysis. Int J Cardiol Heart Vasc 25: 100422, 2019.
27. Hsu S, Houston BA, Tampakakis E, Bacher AC, Rhodes PS, Mathai SC, Damico RL, Kolb TM, Hummers LK, Shah AA, *et al*: Right ventricular functional reserve in pulmonary arterial hypertension. Circulation 133: 2413-2422, 2016.
28. Li X, Shi K, Yang ZG, Guo YK, Huang S, Xia CC, He S, Li ZL, Li C and He Y: Assessing right ventricular deformation in hypertrophic cardiomyopathy patients with preserved right ventricular ejection fraction: A 3.0-T cardiovascular magnetic resonance study. Sci Rep 10: 1967, 2020.
29. Konstam MA, Kiernan MS, Bernstein D, Bozkurt B, Jacob M, Kapur NK, Kociol RD, Lewis EF, Mehra MR, Pagani FD, *et al*: Evaluation and management of right-sided heart failure: A scientific statement from the American heart association. Circulation 137: e578-e622, 2018.
30. Monteagudo-Vela M, Tindale A, Monguió-Santín E, Reyes-Copa G and Panoulas V: Right ventricular failure: Current strategies and future development. Front Cardiovasc Med 10: 998382, 2023.
31. Ryan JJ and Archer SL: The right ventricle in pulmonary arterial hypertension: Disorders of metabolism, angiogenesis and adrenergic signaling in right ventricular failure. Circ Res 115: 176-188, 2014.
32. Mascherbauer J, Marzluf BA, Tufaro C, Pfaffenberger S, Graf A, Wexberg P, Panzenböck A, Jakowitsch J, Bangert C, Laimer D, *et al*: Cardiac magnetic resonance postcontrast T1 time is associated with outcome in patients with heart failure and preserved ejection fraction. Circ Cardiovasc Imaging 6: 1056-1065, 2013.
33. Puntmann VO, Voigt T, Chen Z, Mayr M, Karim R, Rhode K, Pastor A, Carr-White G, Razavi R, Schaeffter T and Nagel E: Native T1 mapping in differentiation of normal myocardium from diffuse disease in hypertrophic and dilated cardiomyopathy. JACC Cardiovasc Imaging 6: 475-484, 2013.
34. Yeong CC, Harrop DL, Ng ACT and Wang WYS: Global longitudinal strain manually measured from mid-myocardial lengths is a reliable alternative to speckle tracking global longitudinal strain. J Cardiovasc Imaging 32: 35, 2024.
35. Seno A, Antiochos P, Lichtenfeld H, Rickers E, Qamar I, Ge Y, Blankstein R, Steigner M, Aghayev A, Jerosch-Herold M and Kwong RY: Prognostic value of T1 mapping and feature tracking by cardiac magnetic resonance in patients with signs and symptoms suspecting heart failure and no clinical evidence of coronary artery disease. J Am Heart Assoc 11: e020981, 2022.
36. Korthals D, Chatzantonis G, Bietenbeck M, Meier C, Stalling P and Yilmaz A: CMR-based T1-mapping offers superior diagnostic value compared to longitudinal strain-based assessment of relative apical sparing in cardiac amyloidosis. Sci Rep 11: 15521, 2021.